Photocatalytic Wastewater Treatment with Titania Bound to Glass

Major Qualifying Project completed in partial fulfillment of the Bachelor of Science Degree at Worcester Polytechnic Institute, Worcester, MA

Submitted by:
Cody Brooks

Professor John Bergendahl, faculty advisor
Professor Fred Hart, co-advisor

December 16, 2013

Abstract

The objective of this project was to study and evaluate the treatment efficiency of a reactor that utilized titanium dioxide (TiO_2) nanoparticles immobilized on glass beads in both a fixed and fluidized bed configuration. The degradation of the organic contaminant, methylene blue, was evaluated with a UV-vis spectrophotometer. Results suggested that the inter-particle forces acting between coated glass beads in a fluidized bed exceeded the bond strength of the nanopowder coating and thus detached. Conversely in a fixed bed, with a lower fluid flow rate, results showed a steady reduction in methylene blue concentration over time when the immobilized titania was exposed to UV irradiation. This degradation was found to perform at a rate much higher than the rate of UV exposure without titania present.

Acknowledgements

This Major Qualifying Project could not have been started and completed without the continual guidance and support from my advisor Professor John Bergendahl. Also, thanks to Professor Frederick Hart and Jose Ricardo Alvarez Corena for their help and guidance during the project and to Abigail Charest for all her guidance in the lab.

Table of Contents

Abstract iii

Acknowledgements iv

Table of Contents v

Table of Figures viii

Table of Tables viii

Executive Summary ix

Design Statement x

1 Introduction 2

2 Background 4

2.1 Wastewater Treatment 4

2.2 Advanced Oxidation Processes 6

2.3 Photochemical AOPs 7

2.3.1 Ultra-Violet (UV) Light 8

2.4 Photocatalytic oxidation 8

2.5 Titanium Dioxide 10

2.5.1 General 10

2.5.2 Photocatalyst 11

2.6 Coating Silica Beads with Titanium Dioxide 14

2.6.1 Attachment using pH Adjustment 14

2.6.2 Dry Mix 15

2.7 Methylene Blue 15

2.8 Summary 16

3 Methodology 17

3.1 Reactor System Setup / Design 17
3.2 Silica Bead Fluidization 19
3.3 Deposition of Titanium Dioxide (TiO_2) onto SiO_2 spheres 19
3.3.1 Dry-Mixing Deposition 19
3.3.2 pH Adjustment Coating Process 20
3.4 Methylene Blue Solution Preparation 21
3.4.1 Methylene Blue Stock Solution 21
3.4.2 Methylene Blue Concentration Standard Curve 21
3.5 Titanium Dioxide & UV Treatment 22
3.5.1 Dry-mix Beads Trial 22
3.5.2 pH Adjustment Beads Trials 23
3.5.3 Uncoated Glass Beads 25
3.5.4 Reservoir water pH adjustment 26
4 Results & Discussion 27
4.1 Calibration Curve 27
4.2 UV Degradation 28
4.2.1 UV Photolysis 28
4.2.2 UV/Dry-mix Beads Degradation 28
4.2.3 UV/pH Adjustment Beads Degradation 29
4.2.4 UV and UV/TiO_2 Degradation Comparison 32
5 Full-scale Design of Ti/UV System 34
5.1 System Design Parameters 34
5.2 Energy Requirements 35
6 Conclusions & Future Work 37
Reference List 38

Appendix A – Glossary of Terms 40

Appendix B – Raw Data 40

Appendix C – System Pictures 46

Table of Figures

Figure 1. Typical wastewater treatment process (Image from Davis, 2009, p. 483). 4

Figure 2. Photo excitation process on a semiconductor particle (Mills, 1997). 9

Figure 3. Tetragonal crystal structure of rutile (Smyth, 1988). 10

Figure 4. Tetragonal crystal structure of anatase (Smyth 1988). 11

Figure 5. Photoinduced processes on titanium dioxide (Carp et. al 2004). 12

Figure 6. Band gap of semiconductors (on left) and redox potentials of several organic functional groups (on right) (Carp et al., 2004). 13

Figure 7. Secondary reactions with activated oxygen species (Hoffman et al., 1995). 13

Figure 8. Chemical structure of methylene blue. 15

Figure 9. System schematic. 17

Figure 10. Glass tube reactor schematic. Figure 11. Attached threaded pieces schematic. 18

Figure 12. Methylene blue standard/calibration curve. 27

Figure 13. UV photolysis degradation. 28

Figure 14. Glass bead bed. Note: TiO_2 coated beads at bottom of bead bed. 30

Figure 15. Methylene blue adsorption and UV degradation in fixed bed of TiO_2-coated glass beads 31

Figure 16. 1st order UV/TiO_2 kinetics in fixed bed of Ti-coated glass beads. 32

Figure 17. MB Degradation of UV vs. UV/TiO_2. 33

Figure 18. 1st order kinetics UV vs. UV/TiO_2. 33

Figure 19. Proposed Flow Schematic. 34

Figure 20. Proposed Reactor Schematic. 35

Table of Tables

Table 1. Relative oxidation power of some oxidizing species (adapted from Munter 2001) 7

Table 2 Physical and chemical properties of methylene blue (Miclescu & Wiklund, 2010) 16

Table 3. MB standard curve samples. 22

Executive Summary

The purpose of this study was to evaluate the treatment efficiency of a reactor that utilized a photochemical advanced oxidation process (AOP) with titanium dioxide (TiO_2) nanoparticles immobilized on glass beads in both a fixed and fluidized bed configuration in order to produce hydroxyl radicals. This photochemical AOP produces nonselective hydroxyl radicals through the photo-excitement of TiO_2 electrons and the oxygen present in the water as the oxidant. Unlike other forms of treatment that transfer contaminants from one phase to the other, UV/TiO_2 AOP's, among others, breakdown the contaminants to non-toxic organics and mineral acids. This bench-scale study focused on determining the degradation rate of the organic contaminant methylene blue and was evaluated through chemical analysis with a UV-vis spectrophotometer and quantified using first order kinetics.

Results suggested that the inter-particle forces acting between coated glass beads in a fluidized bed exceeded the bond strength of the nanopowder coating and thus detached. It was found that the detachment was lessened when the system pH was adjusted to 4.5, the pH used by one of the utilized deposition methods. Conversely in a fixed bed, and lower flow rate, results showed a steady degradation of methylene blue over time when exposed to UV irradiation. UV/TiO_2 degradation was found to perform at a rate much higher than the rate of methylene blue degradation when only exposed to UV light with no TiO_2 present.

It is recommended that further research be performed on the deposition methods, the strengths of the bonds created during deposition, and the forces acting on the coated glass beads within the reactor.

Design Statement

This project fulfills the requirements for the Major Qualifying Project (MQP) in the Civil Engineering Department at WPI by incorporating a design component..

The goal of this project, as stated in the previous section, was to determine the treatment efficiency of a reactor that utilized a photocatalytic AOP with titanium dioxide immobilized on silica beads for removing the organic contaminant methylene blue from the water utilizing a fluidized and fixed bed. The goal of the research was to characterize and quantify the rate at which this photocatalytic reactor would be able to treat the water at bench-scale conditions so that design of a small full-scale reactor could be completed.

First, procedures for deposition of titania onto the silica beads was researched and carried out. Second, laboratory experiments were designed to test both fluidized and non-fluidized beds of Ti-coated silica beads. Experiments were also designed in order to determine the treatment efficiency of both beds. Data obtained from the bench-scale experiments was used in order to design a reactor for a full-scale treatment system treating 25,000 gallons per day of contaminated water. The UV reactor was sized for this application and energy requirements determined. Finally, recommendations were provided for future research and experiments of the fluidized bed reactor of titanium coated silica beads.

1 Introduction

Within the last 20 years, and more specifically with-in the last decade, there has been quite a lot of attention on advanced oxidation processes (AOPs) and their use in water treatment. This attention has come from the potential of these processes to be highly effective at degrading contaminants and waste in water, while introducing little, if any, new harmful substances. This prospect is especially attractive since other processes, such as waste incineration and landfilling, may result in the harmful release of toxic compounds into the environment (Munter 2001). Additionally, some of these common processes only change the phase of the pollutant without actually destroying it such as is the case with air stripping and carbon adsorption processes (Serpone 1995). Thus a lot of research has shifted towards processes in which the contaminants are destroyed and mineralized as phase change isn't truly solving the problem.

Unfortunately these processes presently introduce higher costs to the treatment process, which severely limits their implementation into current systems. As stated by Munter, (2001) "…wide marketing of commercially available solar detoxification systems is obstructed by the general market situation: a new water treatment procedure has an opportunity to be implemented only when its cost is at least two-fold lower than the cost of a procedure currently in use." These high costs stem from a multitude of process specific factors such as, the continuous need for expensive chemical reagents or the higher energy cost associated with powering a UV light source(s) if not already used in the treatment process. Nonetheless the potential for these effective and environmentally friendly systems and processes is there and continued research to solve these high cost drawbacks is essential.

Photocatalytic oxidation systems are one such advanced oxidation process that has garnered increasing popularity. Harada et al. (1999) stated, "…the design of highly efficient photocatalytic systems is of vital interest and one of the most desirable yet challenging goals in the research of environmentally friendly catalysts". Photocatalytic oxidation involves the photo-excitation of a semiconductor resulting from the adsorption of electromagnetic radiation. The semiconductor is excited by photons with enough energy to cause an electron from the valence band to move to the conduction band leaving behind a

positive hole in the valence band. These valence band holes and the hydroxyl radicals produced from the photo reaction induce reduction and oxidation reactions that subsequently degrade organic material. Furthermore this heterogeneous photocatalysis uses oxygen in the air and water rather than ozone and hydrogen peroxide as the oxidant and can be carried out in ambient conditions, making it more appealing.

Though these photocatalytic oxidation systems can effectively degrade organics in the water to non-harmful compounds such as H_2O and CO_2, they too come along with higher energy costs to power the UV lights and higher material costs involved with the selected catalyst. These systems also frequently use the catalyst in a slurry form with the wastewater and must then undergo additional treatment in order to remove the catalyst from the water costing more money and increasing the treatment time. This project aims to research the effectiveness of contaminant removal in a photocatalytic system by attaching the catalyst, titanium dioxide in powder form, to glass beads and exposing them to UV light in a fluidized bed.

2 Background

This chapter provides a brief background on the current water treatment methods and their shortcomings and subsequently a description of how AOPs work, where AOPs fit into this treatment process and why their potential to be used in water treatment is so high and desirable.

Furthermore this chapter provides a more in depth description of AOPs, designated as photochemical, that utilize ultra-violet light energy to help drive the oxidation reactions as well as the specific AOP selected for this project, photocatalytic oxidation, which employs ultraviolet light and the catalyst titanium dioxide (TiO_2). This is followed by a background on the novel approach to coating the photocatalyst TiO_2 to silica beads. Finally this chapter introduces the contaminant methylene blue, whose degradation will be studied.

2.1 Wastewater Treatment

Current treatment of wastewater typically follows a process like the one shown in Figure 1 and is broken down into three main sections which are, primary treatment, secondary treatment and disinfection.

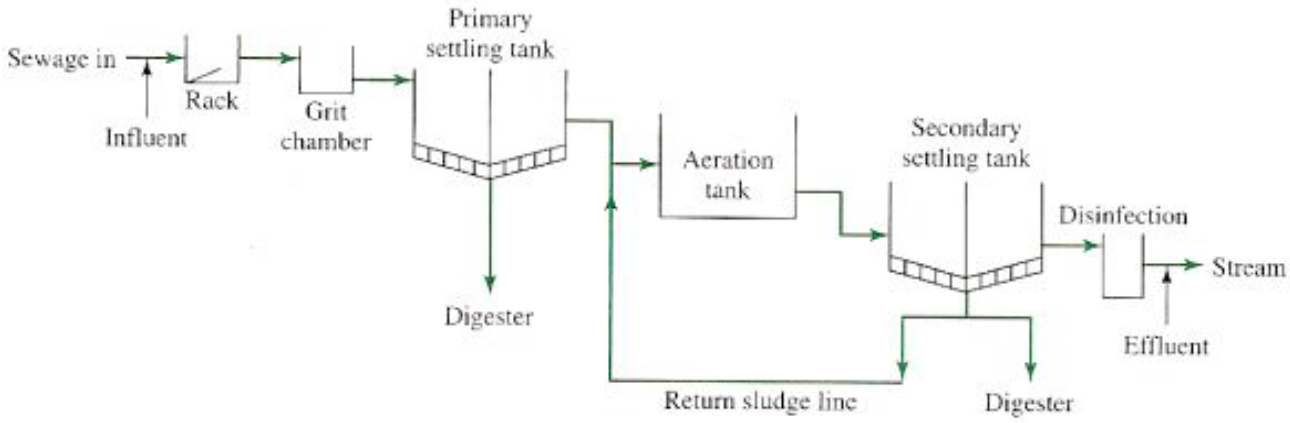

Figure 1. Typical wastewater treatment process (Image from Davis, 2009, p. 483).

The influent enters the system, first passing through a bar rack and grit chamber to catch and settle out any large or readily settled items so as not to damage or hinder any of the subsequent treatment processes or their components. From here the wastewater will

flow into a settling or sedimentation tank that will allow for most of the suspended solids to settle out by gravity as the water slowly flows through it. The sedimentation tank will normally remove about 60% of the suspended solids in raw sewage and reduce the biochemical oxygen demand (Davis, 2009, p. 473). This biochemical oxygen demand (BOD) is a measure of the oxygen used by the microorganisms in the water as they consume the organic material for food; a high BOD indicates a high amount of organic material in the water. The treatment processes are trying to remove this organic material, thus lowering BOD. This sludge that collects on the bottom is pumped out and sent to a digester and eventually will become solid waste. This solid waste will be discussed in later sections of this chapter. The three aforementioned processes makeup the primary treatment phase of the treatment process and from here the water flows into the secondary treatment phase.

In order to remove the remaining colloids and dissolved organics and inorganics, secondary treatment commonly utilizes microorganisms present in the water, which use these dissolved organics as a food source. From the aforementioned primary settling tank the water will usually flow into an aeration tank in order to supply the microorganisms present with oxygen so that they will then begin to breakdown the dissolved organics as food and become what is known as activated sludge. From the aeration tank the water and activated sludge flow into a secondary settling tank allowing for what is called the biomass to settle at the bottom which contains the microorganisms, their food, and products of their digestion. This biomass is then partially recycled into the aeration tank, to ensure a sufficient microorganism population in the system, while the remaining biomass is sent to be digested with the sludge collected from the primary settling tank. While primary and secondary treatment removes most of the solids and unwanted organics that would cause harm to receiving waters, there are still contaminants, pathogens, and other inorganics not dealt with in the first two treatment phases. This is where disinfection is applied.

The most common method of disinfection involves the addition of chlorine to the water in order to disinfect it. Chlorine use arises from its ability as a strong disinfectant and its reasonable cost making it a prime candidate for municipal water treatment, however there are well known drawbacks to its use. These drawbacks include its potential to form chlorinated disinfection byproducts after leaving the treatment system, its toxicity to fish and other biota at low concentrations and its recent rise in cost. Due to these

drawbacks, there has recently been an increase in the use of ozone (O_3) and ultra violet light. These forms of disinfection have become more popular since they disinfect without adding anything to the water being treated and have started to become economically competitive with chlorine disinfection. Furthermore these two disinfectants are being used in conjunction with other chemicals or each other in what are known as advanced oxidation processes or AOPs.

2.2 Advanced Oxidation Processes

Glaze et al. defined AOPs as, "treatment processes which involve the generation of hydroxyl radicals in sufficient quantity to affect water purification". The hydroxyl radical is a powerful and non-selective chemical oxidant that reacts with almost all organic compounds (Munter 2001). Munter explains the organic degradation in stating, "The attack by the OH radical, in the presence of oxygen, initiates a complex cascade of oxidative reactions leading to the mineralization of the organic compound…For example, chlorinated organic compounds are oxidized first to intermediates, such as aldehydes and carboxylic acids, and finally to CO_2, H_2O, and the chloride ion. Nitrogen in organic compounds is usually oxidized to nitrate or to free N_2, sulphur is oxidized to the sulphate."

The non-selectivity of the hydroxyl radical is one of its most attractive characteristics since once it is created it will react immediately with the organics around it. Table 2.3 below taken from Rein Munters paper, *Advanced Oxidation Processes – Current Status and Prospects*, shows the relative oxidation power of hydroxyl radicals and other oxidizers.

Table 1. Relative oxidation power of some oxidizing species (adapted from Munter 2001).

Oxidizing Species	Relative oxidation power
Chlorine	1.00
Hypochlorous acid	1.10
Permanganate	1.24
Hydrogen peroxide	1.31
Ozone	1.52
Atomic oxygen	1.78
Hydroxyl radical	2.05
Positively charged hole on titanium dioxide	2.35

When compared to other oxidizers, hydroxyl radicals are quite powerful. For purposes of this project, note the two species used in this project have the highest relative oxidation power, larger than the oxidation power of other commonly used oxidizer in AOPs, e.g. ozone. With its powerful oxidation and non-selectivity it is apparent why so much research is going into the development of these advanced oxidation processes.

At the moment, there are still economic drawbacks to AOPs that must be solved before they become commonly used on a large scale. AOPs that utilize ozone or UV require large amounts of electricity especially when using them in large scale municipal water treatment. Those utilizing a catalyst continuously consume large amounts of the catalyst which, are commonly expensive and when using them in slurry form require extra treatment to remove the catalyst downstream. Finally there are some AOPs, like the Fenton system, that have a narrow range of pH that must be maintained in order for the process to function; this results in having to buy substances to change and maintain the pH of the water.

2.3 Photochemical AOPs

Photochemical processes are AOPs that utilize ultra-violet (UV) light energy to help drive oxidation reactions to completion. Non-photochemical AOPs, such as those using ozone or hydrogen peroxide, may not completely oxidize organics to carbon dioxide and

water. There are even cases where the intermediate oxidation products are more toxic than the initial reactants (Munter 2001). Photochemical methods include ozone-UV radiation, hydrogen peroxide-UV radiation, ozone-hydrogen peroxide-UV radiation, photo-Fenton systems, and finally photocatalytic oxidation. Adding UV exposure to the treatment process can drive these oxidation reactions to completion since many organics adsorb UV energy causing photolysis, or become excited reacting more easily with chemical oxidants such as ozone and hydrogen peroxide.

2.3.1 Ultra-Violet (UV) Light

Ultra violet light is a non-visible light with wavelengths ranging from 100 nm to 400 nm. These wave-lengths are slightly longer than X-rays and slightly shorter than part of the visible light spectrum. UV light has a few uses within water treatment due to certain wave-lengths of ultra violet light and the radiation they emit (optimum 250 – 270 nm) being able to penetrate the cell wall of an organism as well as its photo-excitation abilities. Once the cell wall has been penetrated the UV radiation affects the DNA and RNA of the microorganism's cell and destroys its ability to reproduce (EPA 1999). This effectively kills the microorganism. This ability to kill off pathogenic organisms without adding chemicals to the water has made it an attractive disinfection method for some time, as long as the cost of powering the UV lamps does not exceed the cost of other disinfection methods. More recently, as stated above, it has been used to drive oxidation reactions to completion in AOPs.

2.4 Photocatalytic oxidation

The process of photocatalytic oxidation or photocatalysis involves the excitation of a semiconductor by the adsorption of electromagnetic radiation, most commonly in the UV spectrum. This semiconductor is excited by photons possessing enough energy to excite electrons from the valence band across what is known as the band gap, to the conduction band. As seen in Eq. 1 using TiO_2 as the example, this results in a negative charge in the conduction band and a positive hole in the valence band, both of which readily induce reduction and oxidation.

$$TiO_2 \xrightarrow{hv} e_{CB}^- + h_{VB}^+ \qquad (1)$$

Figure 2 depicts some of the main processes occurring on an excited semiconductor where, (a) is the electron-hole generation; (b) oxidation of donor; (c) reduction of acceptor; and finally (d) and (e) depict the electron-hole recombination (Carp et al., 2004).

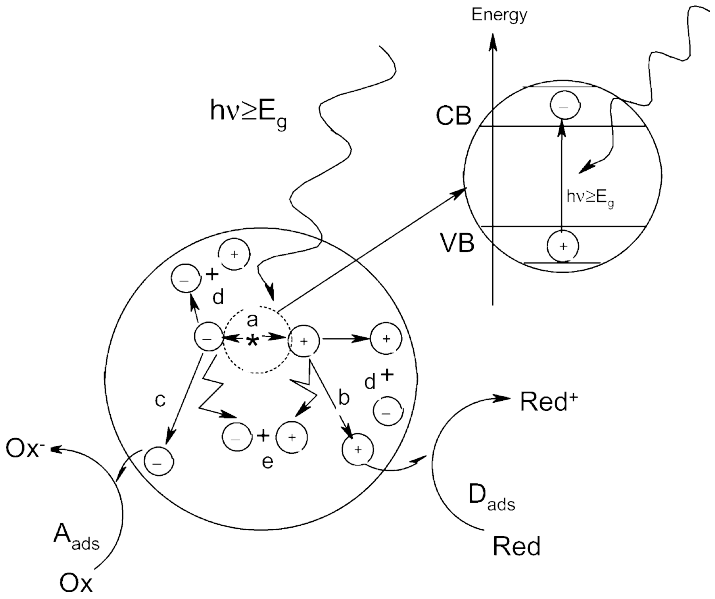

Figure 2. Photo excitation process on a semiconductor particle (Mills, 1997).

Limiting the recombination of the electron-hole is an essential part towards the efficiency of photocatalytic oxidation processes since simply, if there is recombination the semiconductor particle will not take part in the reduction or oxidation of organics and inorganics present. A generalized photocatalytic oxidation reaction on an organic pollutant is given in Eq. 2 showing the non-harmful products of the reaction.

$$\text{Organic Compound} + TiO_2 \rightarrow^{h\nu > Eg} \rightarrow CO_2 + H_2O + \text{mineral acids} \qquad (2)$$

It should be noted this is a generalized reaction equation and there are intermediary products that are produced during the breakdown from organics to mineral acids. The specific intermediates that are formed depend on the contaminants being degraded. From studies performed, while not all intermediates have been researched and documented overall it is found that photocatalytic oxidation processes in general are capable of complete mineralization of many toxic contaminants and they are the most promising heterogeneous photocatalytic applications (Carp et al., 2004).

2.5 Titanium Dioxide

This section highlights the chosen photocatalyst for this project, titanium dioxide, also known as titania or simply TiO_2, and gives a general background.

2.5.1 General

Titanium is the ninth most abundant element on earth and since it is not found unbound to other elements it is primarily found in minerals like rutile, ilmenite, leucoxene, anatase, brookite, and in many iron ores.

Titanium dioxide has been increasingly researched and studied because of its chemical stability, non-toxicity, and low cost. Titanium dioxide is in the transition metal oxides family and is primarily used in paints; roughly 51% of its total production. It is also used in plastics, paper, sunscreen, and is even approved for some applications as a food additive or coloring. International titanium dioxide production exceeds 4 million tons annually (Carp et al., 2004).

Rutile is titanium dioxide's primary ore as it consists of ninety-three percent TiO_2. Figure 3 below displays rutile's tetragonal structure where studies have shown it is titanium dioxide's most stable form.

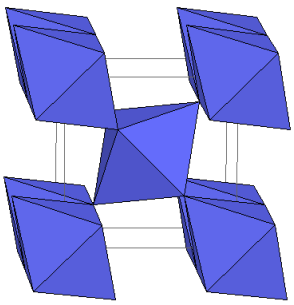

Figure 3. Tetragonal crystal structure of rutile (Smyth, 1988).

Anatase, see Figure 4 for its crystal structure, is a second form of TiO_2 and while both rutile and anatase are used as photocatalysts, anatase has a higher photocatalytic activity in most reactions. Possible explanations for this come from the energy structure of the rutile and anatase type.

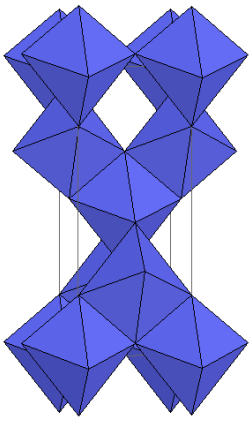

***Figure 4. Tetragonal crystal structure of anatase* (Smyth 1988).**

Both show strong oxidative power from their valence bands yet show a weaker ability for reduction due to their conduction bands being positioned near the redox potential of hydrogen. Since the conduction band in anatase is slightly closer to the negative position, anatase has a slightly higher reduction power (TBTN 2004). There are also studies that have found a combination of rutile and anatase to have a higher activity than pure anatase, such as with the case of Degussa P25. Degussa P25 is a commercially made TiO_2 photocatalyst with an approximate 80/20 ratio of anatase to rutile. This product has been found for many reactions to have a higher photocatalytic activity than either of the pure phases. This is believed to be from an increase in efficiency of the electron-hole separation (Carp et al., 2004).

2.5.2 Photocatalyst

Figure 5 seen below shows the photoinduced process paths for TiO_2. All these paths begin with the excitation of a TiO_2 electron from the valence band (VB) to the conduction band (CB).

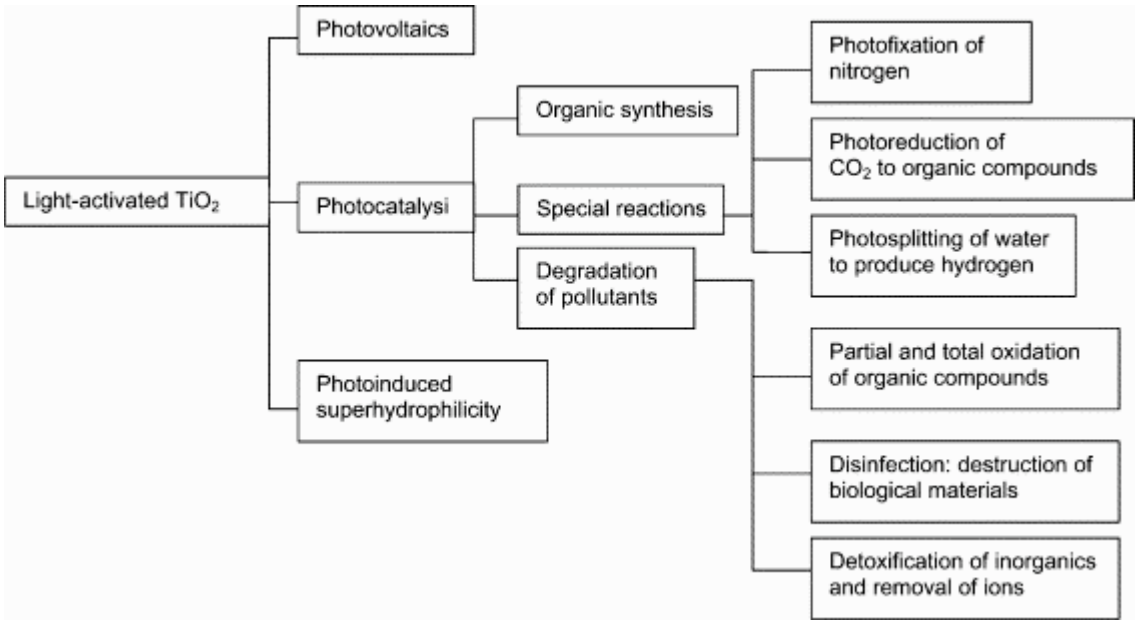

Figure 5. Photoinduced processes on titanium dioxide (Carp et. al 2004).

Carp et al. went on to further state, "Ideally, a semiconductor photocatalyst should be chemically and biologically inert, photocatalytically stable, easy to produce, and to use, efficiently activated by sunlight, able to efficiently catalyze reactions, cheap, and without risk for the environment or humans." TiO_2 is inert, is an efficient catalyst and as stated in the previous section, is abundant, easy to produce through well-established production methods for paints and other products, is non-toxic, and becoming relatively inexpensive. The only area it fails is that it does not adsorb visible light.

The energy needed to excite an electron across the band gap, the area between the valence band and the conduction band, of rutile is 3.0 electron volts (eV) while anatase has a value of 3.2 eV, both of which only absorb ultraviolet light. Figure 6 displays the band gap of several semiconductors as well as showing the redox potentials of some organic functional groups. The white boxes represent the lower edge of the conduction band and the gray boxes represent the upper edge of the valence band. In order for the redox reaction on an adsorbent to take place its redox potential must fall within the lower and upper edge of the conduction band and valence band respectively.

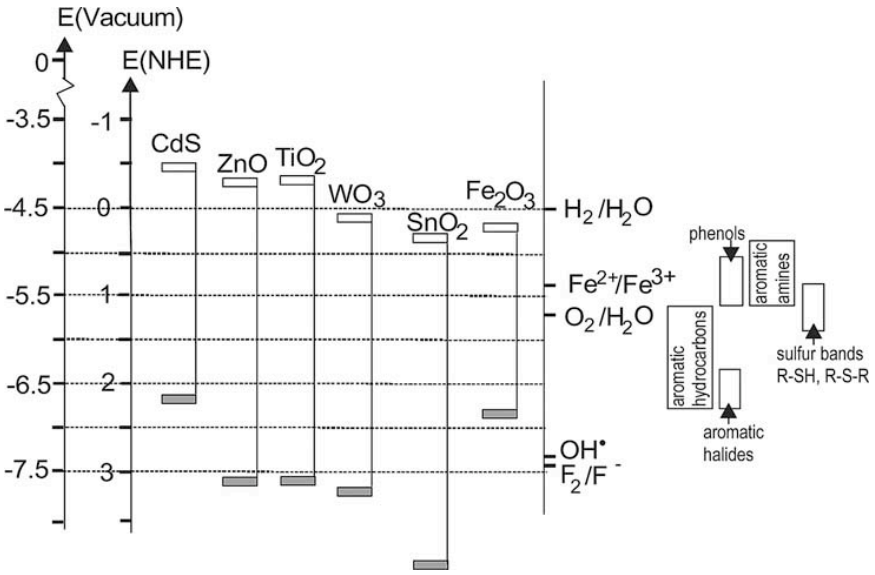

Figure 6. Band gap of semiconductors (on left) and redox potentials of several organic functional groups (on right) (Carp et al., 2004).

As stated by Carp et al., (2004), "TiO_2 has become a photocatalyst in environmental decontamination for a large variety of organics, viruses, bacteria, fungi, algae, and cancer cells, which can be totally degraded and mineralized to CO_2, H_2O and harmless inorganic anions". Figure 7 depicts some of the secondary reactions that can occur after the photo-excitation of TiO_2 including production of hydroxyl radicals and oxidized species on their path towards mineralization.

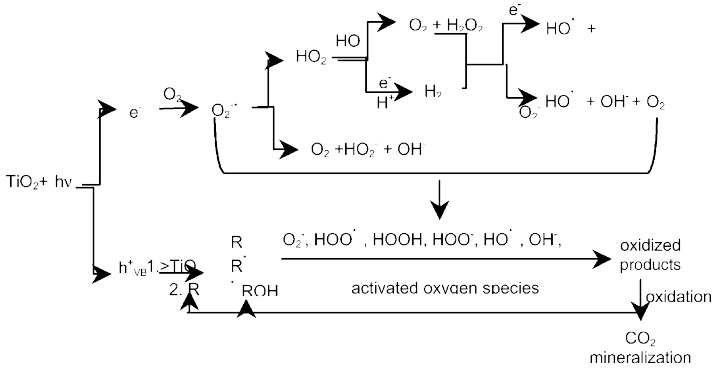

Figure 7. Secondary reactions with activated oxygen species (Hoffman et al., 1995).

One area that is up for debate is titanium dioxide's non-selective oxidation. This trait can be advantageous as it will effectively react and breakdown everything present in the water. However to some this is seen as a disadvantage, since the non-selectivity means that the catalyst will not differentiate between hazardous contaminants and pathogens and

those of low toxicity (Carp et al., 2004). Furthermore Carp et al. explains how biological treatment, like that commonly used in wastewater treatment today, can degrade contaminants of low toxicity yet extremely hazardous contaminants are mainly non-biodegradable. Thus currently, to some it would be better if a new treatment system were able to focus on the highly toxic contaminants. Conversely some believe it would be of better interest if the efficiency of a photocatalyzed system was focused on for research and improvement over focusing on narrowing the selectivity of the system. As seen from this point of view, it would be better to have a new system that is able to degrade all contaminants present quickly and efficiently rather than a new system that is essentially just adding on to the current decontamination systems.

2.6 Coating Silica Beads with Titanium Dioxide

Typically, many studies of photocatalytic reactors have used TiO_2 in its powder form either suspended in the water being treated, which must then undergo further processes downstream to remove the TiO_2, or immobilized onto a support, such as those listed by De Lasa et al. on page 20. This study used TiO_2 immobilized onto small glass beads in the photocatalytic reactor. Anchoring of the substrate onto a support is usually done through physical surface forces or chemical bonds (De Lasa et al, 2005). For this project, two methods of immobilization of the substrate onto the support were used consisting of attachment using pH adjustment, adapted from Ryu et al. 2003, and a dry-mix method adapted from Pozzo et al. 1999.

2.6.1 Attachment using pH Adjustment

The method adapted from Ryu et al. simply uses the charge difference between the reactants in order to anchor the TiO_2 onto the silica spheres. As found in the Ryu et al. study the maximum charge difference between the TiO_2 particles and the silica spheres was found to be at a pH of 4.5. Thus this method simply entails pH equalization of the silica solution and TiO_2 solution at a pH below 4.5 and the subsequent mixing and addition of a base in order to adjust the pH of the mixed solution to 4.5. Ryu et al. as well as this study, utilized nitric acid and sodium hydroxide as the acid and base to adjust the solution pH

respectively. After equalization and mixing for an allotted time the beads were simply allowed to dry by evaporation overnight.

2.6.2 Dry Mix

The method adapted from Pozzo et al. consisted of weighing out predetermined amounts of silica beads and TiO_2, extended dry mixing in a barrel revolving mixer, rehydration of the silica TiO_2 mix, followed by several heating and calcination steps in order to dry and anchor the TiO_2 to the silica beads.

2.7 Methylene Blue

This study has chosen methylene blue to be used as the contaminant and degradation indicator. It has been chosen since it is organic, inert and non-toxic, and it is a constituent where the degradation was easily tracked and calculated.

Methylene blue, whose chemical structure can be seen in Figure 8, is a heterocyclic aromatic chemical compound with the molecular formula: $C_{16}H_{18}ClN_3S$, $3H_2O$ (Miclescu & Wiklund, 2010).

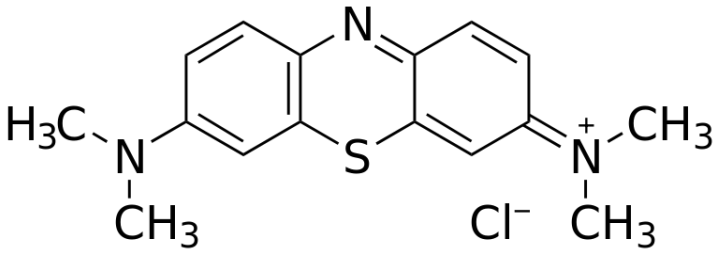

Figure 8. Chemical structure of methylene blue.

Methylene blue is a cationic thiazine dye that has a deep blue color in water when oxidized and colorless when reduced to what is known as leukomethylene blue. Table 2 gives some physical and chemical properties of methylene blue.

Table 2 Physical and chemical properties of methylene blue (Miclescu & Wiklund, 2010).

Physical and chemical properties	Values
Melting Temperature	180°C
Solubility in water	35.5 g/l
pH value	3
Molecular weight	319 g/mol
Color	Dark blue-green in oxidized form, colorless in reduced form

The methylene blue used in all parts of this study was Fisher Scientific Methylene Blue M-291 with a total dye content of 87%.

2.8 Summary

The potential of advanced oxidation processes and more specifically photocatalytic oxidation systems in water treatment has been realized and therefore much attention has been garnered towards researching and advancing this specific field. The use of TiO_2 as a photocatalyst in these photocatalytic oxidation processes using UV light has been established, however there is still need for research in related areas in order to increase efficiencies, lower costs, and fully understand the mechanisms at work. The goal of this project was to evaluate the treatment efficiency of a reactor that utilizes TiO_2 nanoparticles immobilized on glass beads in a fixed and fluidized bed configuration. The degradation of the organic contaminant methylene blue was evaluated through chemical analysis with a UV-vis spectrophotometer.

3 Methodology

The purpose of this section is to present all methods carried out during this project. The first part of this section describes the methods for the setup of fluidizing the glass beads in the reactor. The next section presents the methods used in order to coat the glass beads in TiO_2. Following these sections is the methods used in carrying out the contaminant removal experiment, the main experiment of this project whose results are the main focus of analysis and were used in the design.

3.1 Reactor System Setup / Design

In order to begin testing the fluidization of the glass beads a simple system consisting of a reservoir, a peristaltic pump and reactor was setup. Figure 9 shows a schematic of the system.

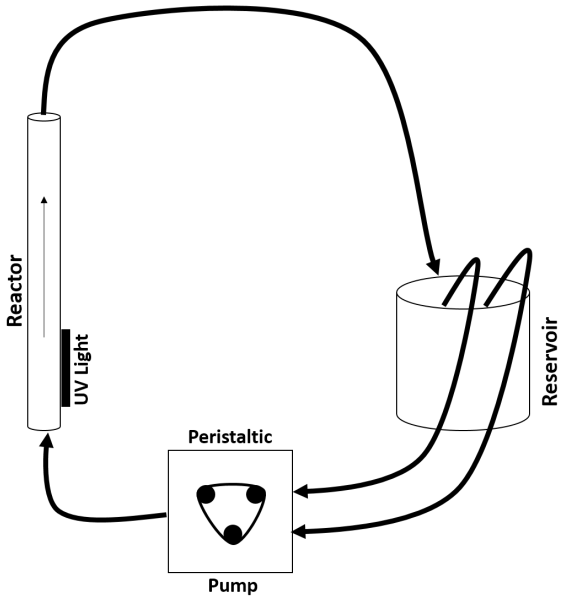

Figure 9. System schematic.

The reservoir was a 2000 mL beaker filled with water and placed on a magnetic stir plate to keep the reservoir continuously stirred. The peristaltic pump's two intake tubes and the reactors outlet tube were placed in the reservoir as well. The peristaltic pump used for all testing and experiments was a Master Flex L/S Digital Standard Drive Model 7518-

00. The reactor in all experiments, as can be seen in Figure 10 consists of a cylindrical glass tube 50.5 cm tall with a 2.5 cm inside diameter and threaded ends.

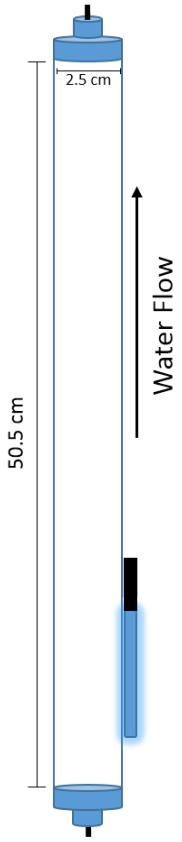

Figure 10. Glass tube reactor schematic.

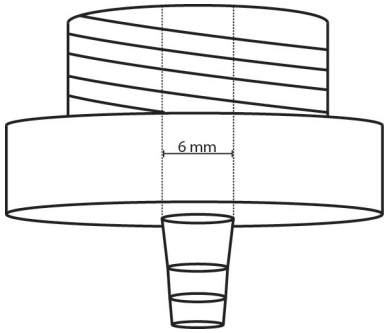

Figure 11. Attached threaded pieces schematic.

Threaded plastic pieces, shown in Figure 11, were screwed into both ends of the glass tube reactor, which had fittings protruding out the opposite ends to which the outlet and intake tubes were attached. The UV source used in all experiments was a Spectroline Model 36-380 Longwave UV (365 nm) pencil bulb connected to a Spectroline Model SCT-1A Power supply and was attached to the outside of the glass reactor tube and surrounded by aluminum foil in order to keep the UV light in the reactor space, as well as for safety. The same clear vinyl tubing was used throughout the system with a 3/8 inch outside diameter, and a 1/4 inch inner diameter. The total tubing length used in the system was roughly equal to 9 feet.

3.2 Silica Bead Fluidization

During the setup of the system described above various trials were run in order to achieve fluidization of the glass beads. Initially 3 mm diameter glass beads were used and several trials were run using beads of this diameter. However, it was found the diameter of these beads was too large and flow rates high enough to fluidize these size beads through the reactor were unattainable. The highest flow rate attainable during these first trials was ~170 mL per minute. In order to achieve higher flow rates a second peristaltic tube was added to the peristaltic pump. To accommodate this, a second inlet tube was attached to the new peristaltic tube and a Y adapter was attached to the outlet of the peristaltic pump so only one tube was feeding into the reactor. Measurements of the flow rate after this change were ~370 mL per minute. This flow rate was still insufficient enough to fluidize the 3 mm diameter beads and so the size of glass beads used was reduced to 425-600 μm. New trials were performed with the finalized setup as described in the above section, along with the new beads and peristaltic pump setup. During these trials, fluidization was achieved where a 27% expansion was measured.

3.3 Deposition of Titanium Dioxide (TiO_2) onto SiO_2 spheres

Presented below are the two methods used in order to coat the silica glass beads with the TiO_2 powder/nanopowder. These include a dry mixing process and a pH adjustment and mixing process. These methods have been adapted from deposition methods used and described by Pozzo et al., and Ryu et al. respectively.

3.3.1 Dry-Mixing Deposition

A fraction of the 425-600 μm glass bead were washed in acetone, in order to remove any organic matter. The beads were placed into a beaker and ~ 30 mL of acetone were added and allowed to mix with the beads for 30 minutes. After this time E-pure water was added to the beaker until almost full and allowed to mix for 5 minutes. Then the beaker was emptied into a vacuum filter apparatus. The beads were kept in the vacuum filter apparatus as the beaker was filled with E-pure water and poured over the beads. This was repeated ~10 times to ensure a thorough rinse. Once rinsing was complete the beads were

transferred into a glass beaker, covered with aluminum foil (vent holes were added to let moisture out), and then placed in an oven overnight at 105° C to allow for complete drying of the beads. After oven drying the beads were weighed out into 4 equal parts of 47.0 g and transferred into 4 amber vials. Predetermined amounts of TiO_2 anatase nanopowder were weighed out and added to the vials. The vials were capped and then placed in a barrel rolling mixer and allowed to mix overnight in order to ensure thorough dry-mixing of the glass beads and TiO_2. After mixing overnight the beads in the vials were removed from the mixer and transferred into 2 beakers, 2 vials of glass beads per beaker. Using a pipette, E-pure water was added to each beaker drop by drop while being stirred with a glass stirrer until a fluid "paste" consistency was reached. Once this consistency was reached the beads were continuously stirred for several minutes. The beakers were then covered with aluminum foil with vent holes and placed in an oven to dry overnight again at 105° C. After drying the beads were removed from the oven and stirred to remove any beads that may be stuck to the beaker. The beakers were then placed in muffle furnace and calcined overnight at 400° C. This calcination was done in order to strengthen the bond between the TiO_2 coating and glass beads, as well as to influence the TiO_2 into its anatase form that has shown a higher photocatalytic activity. Finally, after calcination the beads were taken from the muffle furnace and allowed to cool before use.

3.3.2 pH Adjustment Coating Process

In accordance with the procedures of Ryu et al., the TiO_2/SiO_2 weight ratio for this deposition process was 15%. The Ryu et al. study found this ratio to be ideal for a complete and consistent coating of TiO_2 over the SiO_2 spheres.

First, a fraction of the 425-600 μm glass beads were weighed and found to be 78.0 g. In accordance with the ratio recommended by Ryu et al. this translated to 11.7 g of TiO_2 nanopowder. The glass beads and TiO_2 were transferred into separate beakers, where the TiO_2 container was covered with parafilm during storage. The beaker containing the glass beads was placed on a magnetic stir plate where 30 mL of acetone were added to it and was allowed to mix for 20 minutes. Subsequently the glass beads were thoroughly rinsed by transferring the glass beads and acetone solution to a vacuum filter apparatus where they were rinsed with ~1000 mL of E-pure water.

Once sufficiently rinsed, 40 mL of E-pure water was added to the beaker containing the TiO_2 powder. The pH of this solution was then measured and recorded to be a pH of 2.37. The beaker containing the silica beads also had 40 mL of E-pure water added to it and its pH was also measured. The pH of the silica beads solution was then adjusted down to a pH equal to that of the TiO_2 solution by adding nitric acid drop by drop and intermittently measuring the pH. Once equal, the silica bead beaker was placed on a magnetic stirrer and the TiO_2 solution was added to it. After mixing together the pH of the combined solution was adjusted drop by drop using sodium hydroxide until the combined solutions pH was measured to be 4.49. Once this pH was reached the combined solution was allowed to mix on the magnetic stir plate for 3 hours. Finally, the glass beads were put through vacuum pump filtration in order remove excess water, then spread out on aluminum foil to air dry overnight.

3.4 Methylene Blue Solution Preparation

This section describes the methods for preparing the methylene blue stock solution used throughout all experiments. Furthermore it expresses the method for creating the standard absorption/concentration curve for methylene blue at a wavelength of 664 nm, to be used as the standard for all methylene blue removal analysis.

3.4.1 Methylene Blue Stock Solution

In order for ease and consistency when testing, a stock solution of methylene blue was made. It was decided that a solution of 100 mg/L would be a sufficient concentration. To this point, 100 mg of methylene blue in powder form was added to a 1 L volumetric flask and subsequently filled up to the line with E-pure water. It was then mixed by inversion 5 times to ensure a homogeneous solution. All amounts of methylene blue added to the treatment system were pipetted from this stock solution.

3.4.2 Methylene Blue Concentration Standard Curve

In order to perform analysis on the rate of methylene blue removal a standard curve is needed. In order to achieve this, 7 samples were prepared of varying concentration and their absorbance measured with the spectrophotometer. Table 3.1 presents the

concentrations used and their absorbance. All samples were prepared using the same method.

For preparation of the 1, 3, 5, and 8 mg/L solutions the respective amounts were weighed out and then added to a 1 L volumetric flask. These flasks were then filled to the mark with E-pure water and mixed by plugging and inverting the flask several times. For preparation of the 10 and 15 mg/L solutions, 5 and 7.5 mg of methylene blue powder were weighed out and then added to their own 500 mL volumetric flasks and mixed by inversion several times. From these solutions a pipette was used to transfer some of the solution to a cuvette. These cuvettes were then systematically put into the spectrophotometer, which was set to read at a wavelength 664 nm, where the absorbance was read and recorded. Table 3.1 gives the sample concentrations and their respective measured absorbance.

Table 3. MB standard curve samples.

Concentration (mg/L)	Absorbance (@ 664 nm)	Adjusted Absorbance
0	.0590	0
1	.4276	.3686
3	.5740	.515
5	1.0850	1.026
8	1.5845	1.5255
10	1.9035	1.8445
15	2.5859	2.5269

3.5 Titanium Dioxide & UV Treatment

This section describes the methods used in sampling and testing the removal of the specified contaminant, methylene blue, from the reactor and system described above in section 3.1 by spectrophotometry.

3.5.1 Dry-mix Beads Trial

A portion of the TiO_2 coated beads were weighed out and transferred to the reactor described in section 3.1. Being sure all influent and effluent tubes were in place the

peristaltic pump was turned on and the system was allowed to fill up with water. During this first exposure to running water it was observed that the effluent had a very milky color indicating the presence of slurry form TiO_2, either being excess from the deposition method or un-anchoring from the silica beads themselves. In an attempt to "rinse" the excess TiO_2 from glass beads the effluent tube was removed from the reservoir and placed in a separate large beaker. Then ~2 L of E-pure water was pumped through the system. Once done the effluent tube was placed back into the reservoir to close the loop and the system was started again. In order to see if more TiO_2 was detaching or there was more excess TiO_2, a sample was taken every 5 minutes and its absorbance was read and recorded. After several samples were read it was found that more detached TiO_2 was entering the system.

In an attempt to remedy the detachment of TiO_2, since the dry-mix deposition method beads were used, the pH of the E-pure water being used was brought down to the pH of 4.5, the same used in the pH adjustment deposition method. A short flux was first observed when the pH was adjusted however subsequent sampling indicated that the absorbance was increasing at a much slower rate. At this time, using a volumetric pipette, 10 mL of methylene blue stock solution was added to the reservoir. When the 10 mL of methylene blue stock solution was added an expected trend was observed. The absorbance spiked, as the initial dosage dispersed through the system, followed by slowly diminishing, as the system absorbed the methylene blue. When the absorbance was found to be rising again the UV light was turned on. The system was allowed to run for ~40 minutes, taking samples with plastic cuvettes from the continuously stirred reservoir, and testing absorbance about every 4-5 minutes for the first 20 minutes followed by sample testing about ever 1-2 minutes until system shutdown.

3.5.2 pH Adjustment Beads Trials

3.5.2.1 Trial 1

Due to the detachment of TiO_2 from the glass beads used in the previous trial it was decided that all water used in the trial involving the pH deposition method beads would have its pH lowered to 4.5. This would help to ensure, at least chemically, that the TiO_2 was adequately anchored to the beads.

Once the pH of the reservoir water was adjusted a portion of the beads were weighed (74.2 g) and placed in the glass tube reactor. The first 2 L reservoir had the intake tubes placed in it and the effluent tube was placed in another empty beaker. The purpose of this first run was to "rinse" any excess TiO_2 that was present on the glass beads as well as for observation of how much TiO_2, if any, would come off with the pH adjusted reservoir water. After the system was setup the flow was started, and upon fluidization it was observed that the water turned a very milky color. The second 2 L reservoir of E-pure water was pumped through and it was observed that the water was not getting any less milky, suggesting TiO_2 was still detaching from the glass beads.

At this time it was decided that a fixed, non-fluidized, bed should be tested to see if the stresses and friction involved in fluidization were a factor in the disassociation of the TiO_2 coating from the glass beads. The flow was lowered from ~370 mL/min to a drastically slower 40 mL/min effectively de-fluidizing the bed. The system was closed and the TiO_2 white water was cycled through for 15 minutes to allow for some of the slurry TiO_2 to re-attach to the glass beads. After 15 minutes the TiO_2 water was drained and the third 2 L E-pure water reservoir was placed on the magnetic stirrer. An initial sample was taken from the reservoir water and its absorbance at 664 nm was read and subsequently zeroed. The system was allowed to run at this newly designated flow rate and several samples were taken. The absorbance read from these samples showed a very slow increase in the absorbance overtime suggesting that the TiO_2 present in the system was staying within the packed bed of glass beads and reactor column.

Once this was found, 10 mL of the 100 mg/L methylene blue stock solution was added to the reservoir and samples were taken from the continuously stirred reservoir roughly every 5 minutes. These samples were placed in the spectrophotometer and their absorbance was read and recorded. When the absorbance was found to be rising again the UV light was turned on and sampling continued. After fifteen minutes of operation the flow rate was increased to 50 mL/min in order to increase the amount of water treated yet still keep a non-fluidized bed reactor. Sampling was continued for another hour and fifteen minutes and the absorbance continued to diminish. After this time it was attempted to find the maximum flow rate attainable with no fluidization of the bed and minimal release of the TiO_2 coating. The flow rate was increased until movement in the beads was observed

and samples were taken. It was found that at a flow rate of 70 mL/min slurry from detached TiO_2 was entering the system and the absorbance of the samples spiked. Once the absorbance of the samples were recorded the system was shutdown.

3.5.2.2 Trial 2

A second trial was performed using the pH beads due to the degradation that was found once the system flow rate was reduced. This second trial was performed using the same methods described above and used in the other trials. E-pure water with an adjusted pH was again prepared and placed on the magnetic stirrer and had all tubes placed in it. The system was run at a flow rate of 50 mL/min and initial samples showed the absorbance was not increasing over time. From this point the 10 mL dose of methylene blue stock solution was added and followed its normal trend. The UV was turned on and samples were taken every 15 minutes. This trial was run for a total of 6 hours once the methylene blue solution was added.

3.5.3 Uncoated Glass Beads

A control experiment was performed using only UV and uncoated glass beads to give perspective on how the TiO_2 (alone) affects the system. This trial was performed using a very similar method as the previous trials using coated glass beads.

The system was first rinsed with 2 L of E-pure water and several samples absorbance was read in order to ensure no TiO_2 or MB residue was left in the system. Based on the amount of pH adjustment beads used and accounting for the weight of TiO_2 powder attached, 65 g of glass beads was weighed and added to the glass reactor. In order to rinse the glass beads 2 L of E-pure was pumped through the system and discarded. The reservoir water was replaced with fresh E-pure water and the flow was then decreased to the flow rate used in the previous pH adjustment beads trials of 50 mL/min.

The system was started and subsequently 10 mL of the 100 mg/L methylene blue stock solution was pipetted into the reservoir. Samples were then subsequently taken every 5 minutes and their absorbance was read and recorded. Again the methylene blue followed its normal trend of being absorbed by the system. Once the absorbance was flattening out the UV light was turned on. Samples were then methodically taken every ten

minutes and their absorbance was read and recorded. This system was allowed to run for a total of 2 hours before system shutdown.

3.5.4 Reservoir water pH adjustment

In preparation, three 2 L beakers were filled with E-pure water and one was placed onto a magnetic stirrer and its pH was read. Using a pipette, nitric acid was added to the water drop by drop re-reading the pH between each drop. This method was carried out for all three beakers. Additionally, two of the beakers when being adjusted with nitric acid fell below a pH of 4.5. To solve this, using a pipette sodium hydroxide was added drop by drop until the pH rose to ~4.5. The final pH read and recorded for the three reservoirs was 4.5, 4.46, and 4.51.

4 Results & Discussion

The goal of this project was to evaluate the treatment efficiency of a reactor that utilized TiO_2 nanoparticles immobilized on glass beads in a fixed and fluidized bed configuration. The degradation of the organic contaminant methylene blue was evaluated through chemical analysis with a UV-vis spectrophotometer which was used to determine the degradation reaction kinetics. The data was used to carry out a scaled-up system design as well as to make recommendations for future research.

4.1 Calibration Curve

A calibration curve was created for methylene blue with a UV-vis spectrophotometer at a wavelength of 664 nm. The curve is plotted below in Figure 12.

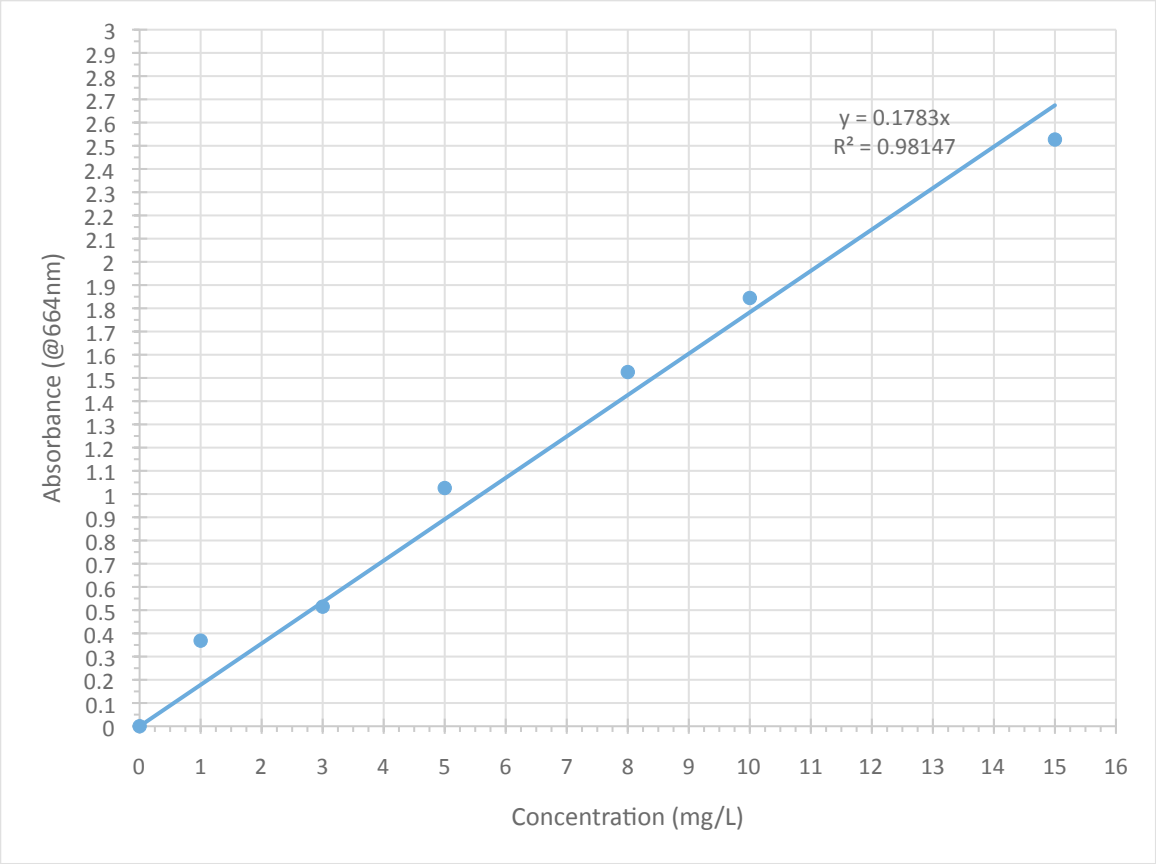

Figure 12. Methylene blue standard/calibration curve.

The data was fit to a line with an R^2 value of 0.9815.

4.2 UV Degradation

4.2.1 UV Photolysis

A UV photolysis trial was run in order to make comparisons of degradation with and without TiO_2 present in the system. Figure 13 shows the reduction of methylene blue concentration over time. As can be seen, the majority of concentration reduction takes place before any UV exposure, which was during the time the system was absorbing the methylene blue. Once UV exposure was commenced the concentration was still decreasing but at a very slow rate.

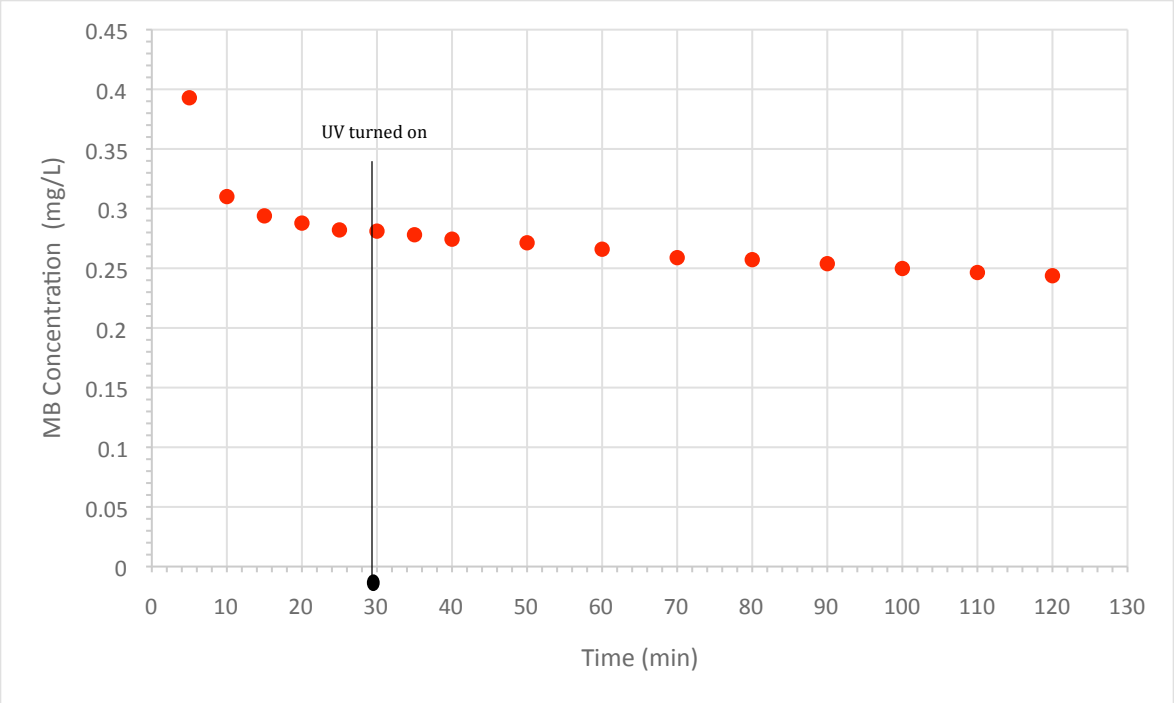

Figure 13. UV photolysis degradation.

4.2.2 UV/Dry-mix Beads Degradation

This first trial (data shown in Appendix B), proved to be an indicator of TiO_2 detachment from the glass beads. During the first few samples the absorbance was increasing at a very fast rate which indicated large amounts of unattached TiO_2 in the glass beads, TiO_2 rapidly detaching from the glass beads, or most likely a combination of both.

Therefore “rinsing” with clean water was performed in order to remove the leftover unattached TiO_2.

During the initial pH adjustment of the reservoir water it was observed that there was a short flux in the amount of TiO_2 released by the beads. However, when the system was allowed to run and samples were methodically taken and their absorbance tested it was found that the absorbance was increasing at a much slower rate. Once this was observed it was decided that an attempt to see how the addition of methylene blue would affect the system and if once exposed to UV light if there would be any breakdown of the methylene blue with the TiO_2 still present in the system.

After the application of the methylene blue dose and allowing the system to undergo UV exposure, as samples were taken, the absorbance continued to rise over the first 20 minute period then began rising and falling between each absorbance reading. This could possibly be explained by more TiO_2 entering the system thus causing the absorbance to rise while conversely, methylene blue degradation was causing the absorbance to go down. These “opposing” forces could have caused the rising and falling numbers that were found. Though overall the absorbance was still rising faster than it was falling meaning TiO_2 was entering the system at a faster rate than the rate of methylene blue degradation.

4.2.3 UV/pH Adjustment Beads Degradation

Though the pH adjustment of the reservoir water lowered the rate at which the TiO_2 detached from the glass beads, it did not solve the problem completely. During this trial it was observed that the coated beads occupying the bottom outer rim of reactor (area of lowest flow rate) were still coated, see Figure 14.

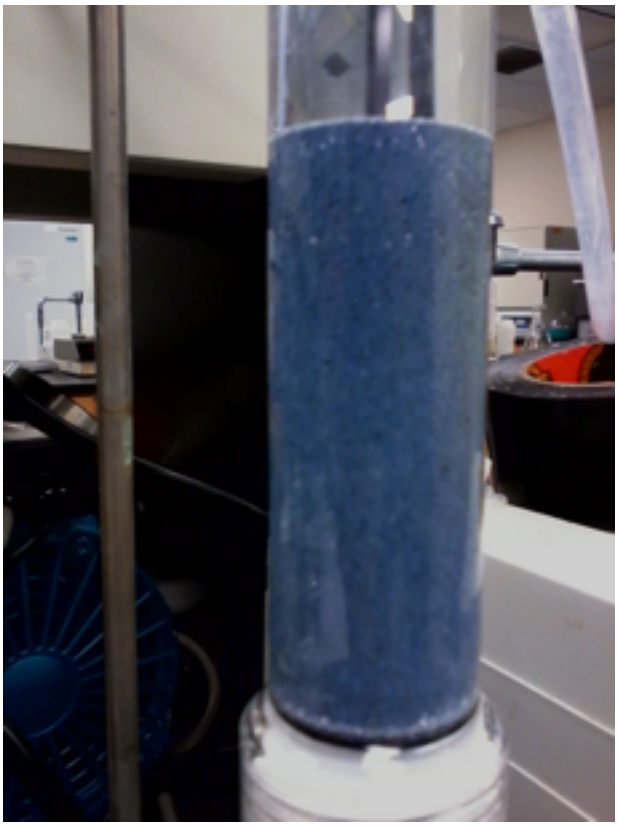

Figure 14. Glass bead bed. Note: TiO_2 coated beads at bottom of bead bed.

This suggests flow rates were too high and the friction caused from rubbing and collision between fluidized beads resulted in the TiO_2 coating detaching and returning to a slurry form in the system water. Basing on the results from the previous trials and the observations made it was decided at that point to reduce the flow to effectively remove the fluidization so as to test the new hypothesis that fluidization forces were too great for the TiO_2 coating to remain attached.

To this point, after flow reduction, adding calculated amounts of methylene blue and exposing to UV light, absorbance trials showed a steady rate of degradation of the methylene blue as can be seen in Figure 15. Starting with an initial concentration dose of 0.45 mg/L of methylene blue the system absorbed roughly .17 mg/L of methylene blue to a concentration of 0.276 mg/L.

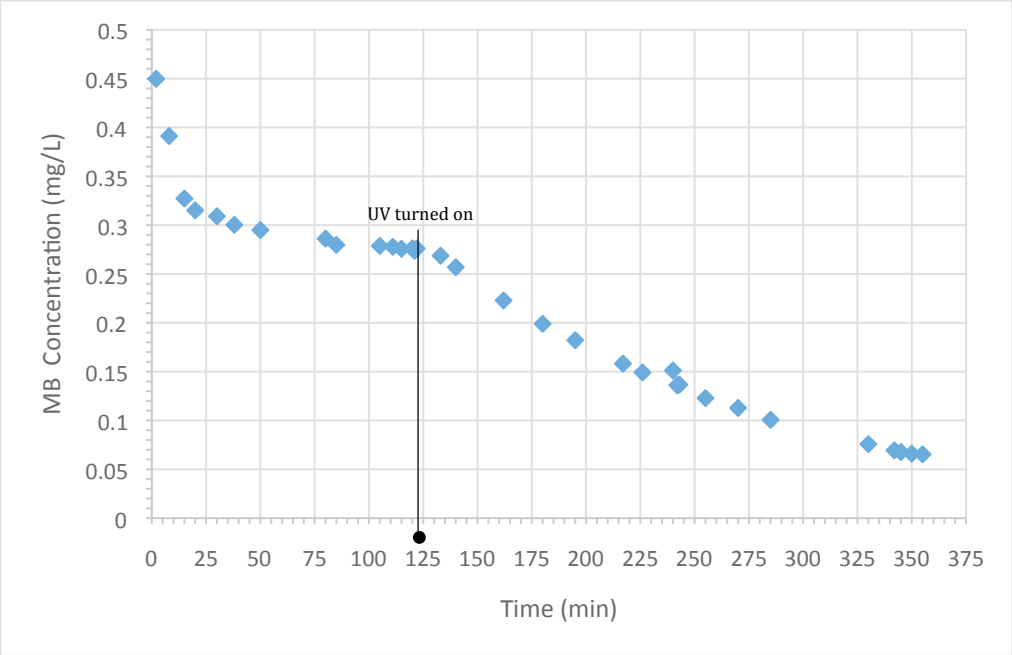

Figure 15. Methylene blue adsorption and UV degradation in fixed bed of TiO_2-coated glass beads.

As can be observed in Figure 15, the system adsorption of methylene blue slowed and began to flatten out around the 125-minute mark. Then, the UV light was turned on and followed an almost linear decline of methylene blue concentration. The final concentration was calculated to be 0.065 mg/L; a reduction of 75.8% from UV/ TiO_2 exposure.

The data collected from these trials were used in Equation 3 in order to calculate the reaction rate constant for the system.

$$-d[MB]/dt = k[MB] \quad (3)$$

Where [MB] = Concentration of methylene blue (mg/L)

t = time (min)

k = rate constant (1/min)

When integrated it becomes Equation 4.

$$ln[MB] = -kt + ln[MB]_0 \quad (4)$$

Solving for *k*, results in Equation 5.

$$k = -(ln[MB] - ln[MB]_0) / t \quad (5)$$

Previous studies (Zaifeng et al. 2000) have shown the photodegradation of methylene blue over TiO_2 particles follows first order kinetics. By graphing the natural log of methylene blue concentration vs. time, the resultant slope of the line is equal to $-k$.

Figure 16 depicts the first order plot of degradation with time equal to zero being when the UV light source was initially turned on. The rate law constant was found to be 0.0065/min (R^2=0.99).

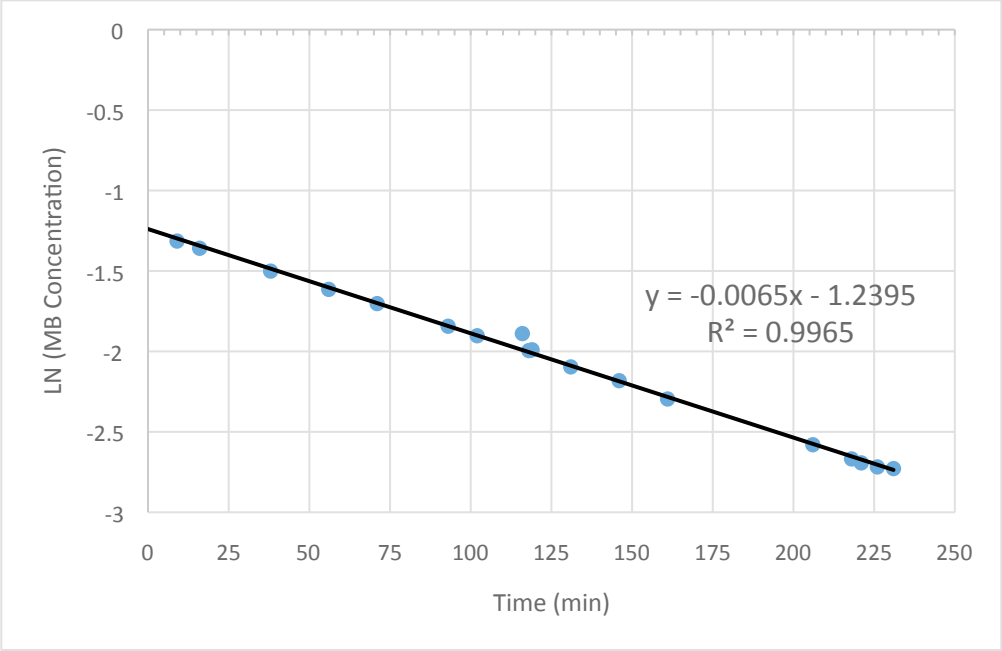

Figure 16. 1st order UV/TiO_2 kinetics in fixed bed of Ti-coated glass beads.

4.2.4 UV and UV/TiO_2 Degradation Comparison

Figure 17 provides direct comparison of UV reduction in methylene blue concentration with and without TiO_2 present. It can be seen in the figure that without TiO_2 present the rate at which it degrades is much lower, further evidenced by Figure 18, which shows the 1st order kinetics of both trials. From these figures the rate law constant of UV photolysis was found to be 0.0016/min, much lower than the 0.0065/min found when TiO_2 is present along with UV exposure.

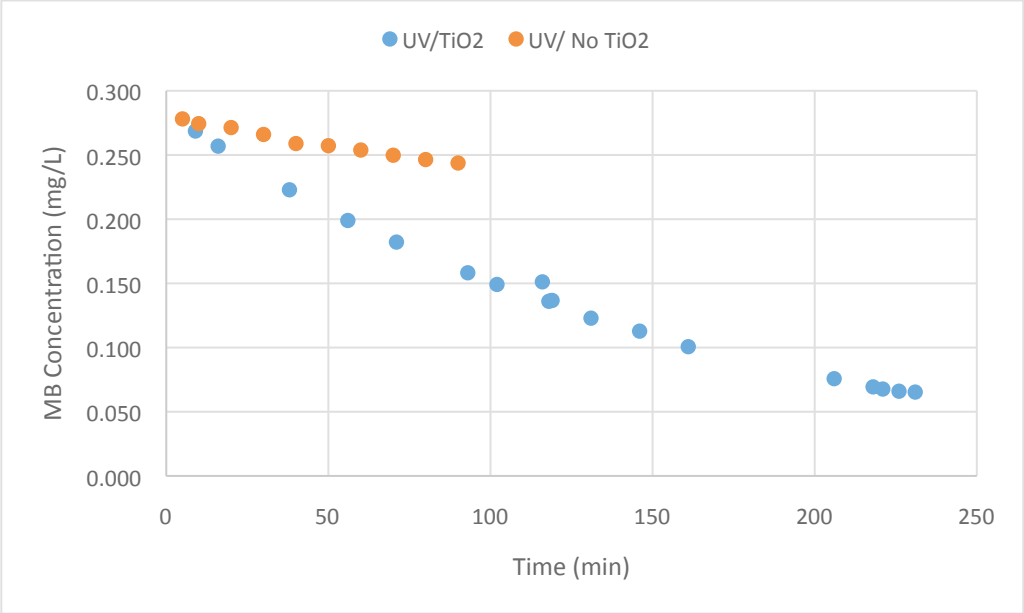

Figure 17. MB Degradation of UV vs. UV/TiO₂.

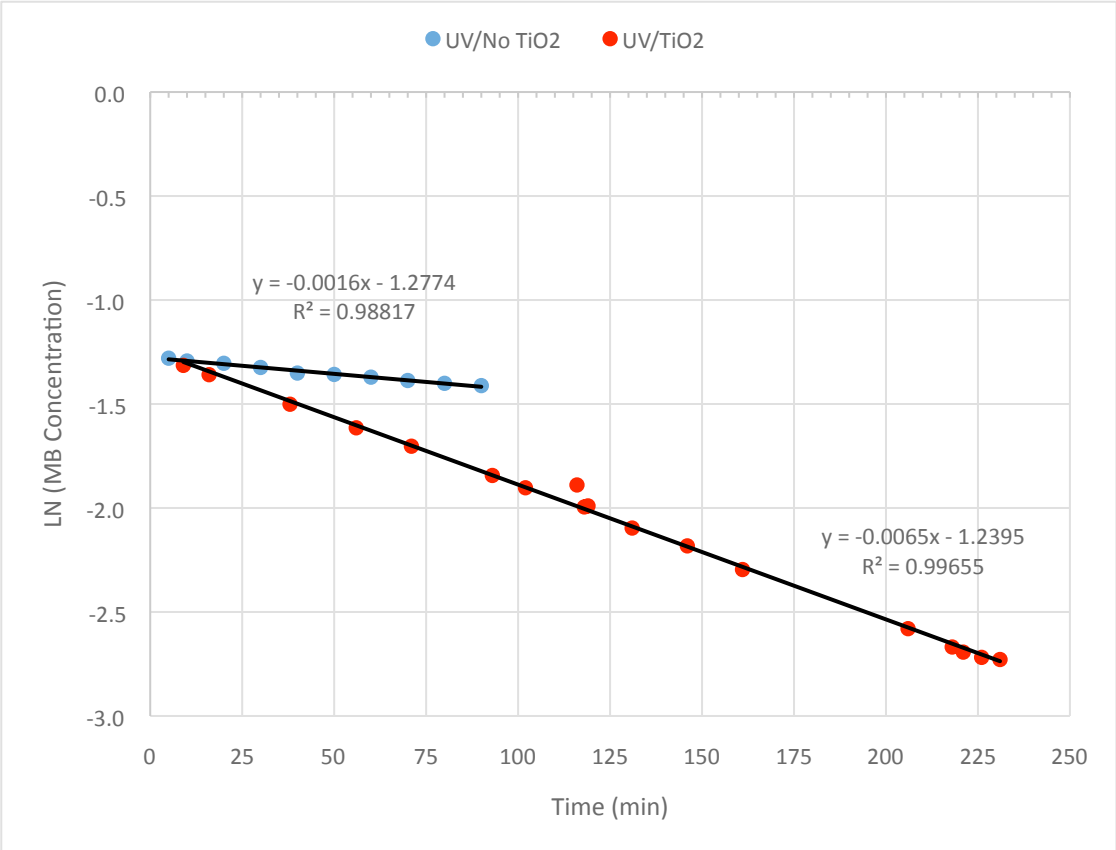

Figure 18. 1st order kinetics UV vs. UV/TiO₂.

5 Full-scale Design of Ti/UV System

This chapter provides considerations for the scaling of the system tested and created in this project. This preliminary design helps to present the system in a more practical application than the bench scale that was utilized for this project.

5.1 System Design Parameters

The design parameters for this situation consist of a maximum flow rate of 25,000 gallons/day (0.0657 m^3/min) of contaminated water with a contaminant concentration of 10 mg/L. Figure 19 below shows the flow schematic for this proposed system. In keeping with materials used during experimentation, for this proposed system Polyvinyl Chloride (PVC) piping was used.

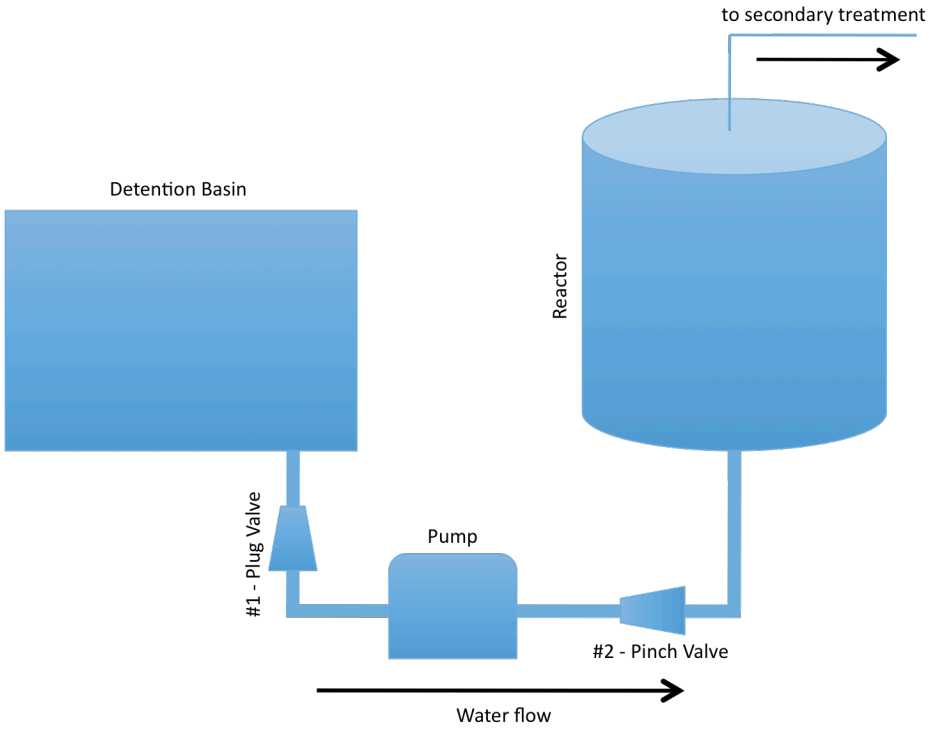

Figure 19. Proposed Flow Schematic.

Scaling to a flow rate of this magnitude was roughly 1300 times larger than the flow rate used during successful experimentation in the lab. With this flow rate, and keeping to a roughly equal fluid superficial velocity of 0.102 m/min in the fixed bed, the reactor dimensions, shown in Figure 20, were calculated. The contactor has a radius of 0.45 m and

a height of 0.51 m, resulting in a volume of 86 gallons (0.326 m^3). When sizing the piping the same diameter ratio of 0.256:1 between the pipe diameter and reactors diameter was kept. With this ratio the inside diameter of the pipes was calculated to be 11.5 cm. As seen in Figure 19, two valves are utilized in order to control the flow rate as well as prevent backflow from the reactor to the pump.

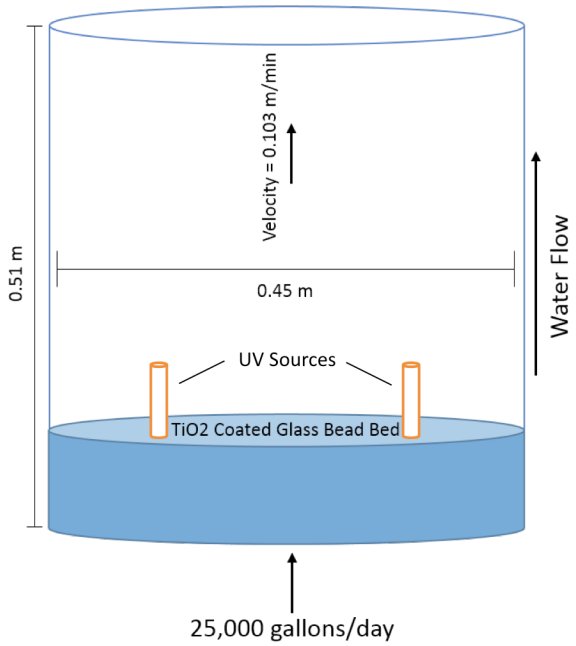

Figure 20. Proposed Reactor Schematic.

Keeping to the scale ratio of 1:1314, the amount of glass beads required was calculated to be 700 g. Using the 15% weight ratio of SiO_2:TiO_2 used in the pH adjustment attachment method, the 700 g of glass beads would require 105 g of TiO_2 powder for coating.

5.2 Energy Requirements

Similar to the physical scaling of the system the same flow rate ratio was used for energy considerations. Calculations, shown below, resulted in finding the energy requirements for the UV source to be 22.7 kW and concurrently the pumps energy requirements to be 332.5 kW.

5.2.1 UV Energy Requirements:

Experimental UV power supply: 115 volts 60 Hz 0.15 Amps

$P_{UV2} = P_{UV1} * 1314.4$

P_{UV1} (Watts) = I (amps) * E (volts) = 0.15 amps * 115 volts

$P_{UV1} = 17.25$ Watts

$P_{UV2} = 17.25$ Watts * 1314.4 = 22.7 kW

5.2.2 Pump Energy Requirements:

Experimental Pump: 115/230 Volts AC; 50/60 Hz; 2.2/1.1 Amps

$P_{P2} = P_{P1} * 1314.4$

P_{P1} (Watts) = I (amps) * E (volts) = 2.2 amps * 115 volts

$P_{P1} = 253$ Watts

$P_{P2} = 253$ Watts * 1314.4 = 332.5 kW

6 Conclusions & Future Work

From work in this study and those previously performed it is apparent that treatment of organics with UV and TiO_2 can be successful and can degrade contaminants in water at a faster rate than UV alone. However, from the results of this project it was found that the inter-particle forces involved in a fluidized bed exceeded the bond strength between the TiO_2 powder and glass beads causing it to detach.

To this point it is recommended that further research and experimentation be done on the methods of TiO_2 attachment to glass in order to quantify the forces acting on fluidized coated beads, and to research alternative attachment methods that may produce a stronger bond between the coating and glass beads used. Furthermore it is recommended that studies be done on hollow glass beads that will float in water. It should be studied whether or not by floating the beads in a reactor and providing downward flow, the force needed to fluidize beads of this type may be less than in an upflow fluidized bed, and thus may employ already established deposition methods. More in depth analysis of the energy and costs associated with these systems should also be performed.

Additionally, there was found to be a noticeable color change in the beads in closest proximity to the UV source but not in the beads furthest away from the UV light source. This gives evidence that the entire bed may not be fully irradiated. If correct, the process may not be fully efficient; it is recommended that another UV source be added to the outside of the reactor and/or the emplacement of a UV source in the bottom center of the reactor therefore being fully encased by the coated glass beads, and the resultant distance from UV source to each glass beads be minimized.

Overall it is recommended that further studies first research other deposition methods, as well as work to increase the strength of bonds using existing deposition methods as further study on fluidized beds will be hindered by detachment of the TiO_2.

Reference List

Al-Ekabi, H., and Serpone, N., 1988, Kinetic studies in heterogeneous photocatalysis. 1. Photocatalytic degradation of chlorinated phenols in aerated aqueous solutions over TiO2 supported on a glass matrix, *J. of Physical Chemistry,* 92:5726-5731.

Carp, O., Huisman, C. L., & Reller, A. (2004). Photoinduced reactivity of titanium dioxide. *Progress in Solid State Chemistry*, 33-177.

Davis, M. L., & Masten, S. J. (2009). *Principles of environmental engineering and science* (2nd Ed.). New York, New York: McGraw-Hill.

Droste, R. L. (1997). *Theory and practice of water and wastewater treatment*. Hoboken, New Jersey: John Wiley & Sons, Inc.

Environmental Protection Agency 1999, *Wastewater Technology Fact Sheet – Ultraviolet Disinfection*, viewed 15 September 2013, <http://water.epa.gov/scitech/wastetech/upload/2002_06_28_mtb_uv.pdf>

Henderson, M., 2011, A surface science perspective on TiO2 photocatalysis. Surface Science Reports, 66:185-297.

Hoffman, M. R., Martin, S. T., and Choi, W., 1995, Environmental applications of semiconductor photocatalysis. *Chemical Reviews,* 95:69-96.

Lakshmi, S., Renganathan, R., Fujita, S., 1995, Study on TiO2-mediated photocatalytic degradation of methylene blue. *J. of Photochemistry and Photobiology A: Chem.,* 88:163-167.

De Lasa, H., Serrano, B., & Salaices, M. (2005). *Photocatalytic reaction engineering*. Springer.

Mills, A., Le Hunte, S., 1997, An overview of semiconductor photocatalysis. *J. Photochemistry and Photobiology A: Chemistry,* 108:1-35.

Miclescu, A., Wiklund, L., 2010, Methylene blue, an old drug with new indications? *J Rom Anest Terap Int,* 17:35-41

Munter, R., 2001, Advanced Oxidation Processes–Current Status and Prospects. *Proceedings of the Estonian Academy of Science: Chemistry,* 50(2):59–80.

Pozzo, R. L., Giombi, J. L., Baltanas, M.A., and Cassano, A.E., 2000, Performance in a fluidized bed reactor of photocatalysts immobilized onto inert supports. *Catalysis Today,* 62:175-187.

Pozzo, R., Baltanas, M.A., and Cassano, A.E., 1999, Towards a precise assessment of the performance of supported catalyst for water detoxification processes. *Catalysis Today,* 54:143-157

Ryu, D. H., Kim, S. C., Koo, S. M., 2003, Deposition of titania nanoparticles on spherical silica. *J. of Sol-Gel Sci. and Tech.,* 26:489-493.

Serpone, N., 1995, Brief introductory remarks on heterogeneous photocatalysis. Solar Energy Materials and Solar Cells, 38:369-379.

Serpone, N., Borgarello, E., Harris, R., Cahill, P., Borgarello, M., and Pelizzetti, E., 1986, Photocatalysis over TiO2 supported on a glass substrate. *Solar Energy Materials.* 14(2):121-127.

Serpone, N., Emeline, A.V., Horikoshi, S., Kuznetsov, V. N., and Ryabchuk, V.K., 2012, On the genesis of heterogeneous photocatalysis: a brief historical perspective in the period 1910 to the mid-1980s. Photochem. Photobiol. Sci., 11:1121-1150

Smyth, J. R. and Bish, D. L., 1988, Crystal structures and cation sites of the rock-forming minerals.

"Titanium-oxide Photocatalyst". *Three Bond Technical News.* January 2004; 62

W.P. Hsu, R. Yu, and E.J. Matijevic, J. Colloid Interface Sci*.* 156, 56 (1993).

Yue, P., Khan, F., and Rizzuti, L., 1983, Photocatalytic ammonia synthesis in a fluidized bed reactor. *Chemical Engineering Science,* 38:1893-1900.

Appendix A – Glossary of Terms

AOP – Advanced Oxidation Process

MB – Methylene Blue

TiO_2 – Titanium Dioxide

SiO_2 – Silica

UV – Ultraviolet irradiation

Appendix B – Raw Data

Dry-Mix Beads 1st Trial - 1st Overall Trial			**Dry-Mix Beads 2nd Trial**		
Sample #	Time	Absorbance (@664nm)	Notes	Time	Absorbance (@664 nm)
1	2:20	0.01		12:35	0.0079
2		0.0681		12:38	0.0076
3	2:25	0.0944		12:40	0.0081
4		0.1162		12:43	0.0097
5	2:30	0.139		12:47	0.013
6		0.1479		12:52	0.0181
7	#6 syringe filtered	0.0031		12:58	0.0244
8		0.1754		1:03	0.0263
9	2:43	0.1883		1:07	0.0291
10	3:00	0.2304	10 mL of MB stock solution added		
System drained and rinsed with 2 L of E-pure				1:09	0.146
11	3:35	Zeroed		1:12	0.1239
12	3:40	0.0116		1:15	0.1183
13	3:45	0.0156		1:18	0.1172
14	3:50	0.02		1:23	0.1179

15	3:55	0.0269	UV turned on	1:25	0.1215
16	4:00	0.0273		1:29	0.1223
17	4:10	0.0308		1:35	0.1227
18	4:20	0.0341		1:40	0.1245
19	4:30	0.0392		1:44	0.1244
20	4:40	0.0403		1:45	0.1273
				1:46	0.1255
				1:47	0.1267
				1:48	0.1259
				1:50	0.1266
				1:51	0.1331
				1:53	0.1272
				1:54	0.1266
				1:55	0.1289
				1:56	0.1285
				2:01	0.1234
				2:03	0.1275

pH Attachment Beads - 1st Trial		
Time (pm)	Time Elapsed	Measured Absorbance
Flow rate = 40 mL/min		
Initial Reservoir Water (E-pure)		0.0008
Res. water once system closed		0.0191
		0.0262
3:30		0.0272
3:30	10 mL of MB stock sol. added	
3:31	0:01	0.1677
3:35	0:05	0.157
3:40	0:10	0.1456

3:45	0:15	0.1438
3:52	0:22	0.142
3:57	0:27	0.1444
UV turned on		
4:00	0:30	0.1544
4:03	0:33	0.144
4:05	0:35	0.1473
4:06	0:36	0.1456
4:07	0:37	0.147
4:08	0:38	0.1451
4:09	0:39	0.1458
4:10	0:40	0.1458
4:15	0:45	0.1455
Flow adjusted to 50 mL/min		
4:20	0:50	0.1441
4:23	0:53	0.1428
4:28	0:58	0.1411
4:32	1:02	0.1432
4:34	1:04	0.1417
4:42	1:12	0.1384
4:48	1:18	0.1353
4:52	1:22	0.1359
4:58	1:28	0.132
5:03	1:33	0.1318
5:08	1:38	0.1286
5:13	1:43	0.1272
5:20	1:50	0.1263
5:25	1:55	0.1241
5:30	2:00	0.125
5:31	2:01	0.1243
Flow adjusted to 70 mL/min		

5:34	2:04	0.1336
5:36	2:06	0.1464
5:38	2:08	0.1486
System Shutdown		

pH Attachment Beads - 2nd Trial					
Time (PM)	Overall Time Elapsed (min)	MB Presence Time Elapsed (min)	UV exposure Time elapsed (min)	Measured Absorbance	Concentration (mg/L)
1:03	0			0.0012	
1:10	7			0.0052	
1:15	12			0.0075	
1:22	19			0.0051	
1:27	24			0.0057	
1:30	27	0		10 mL MB stock solution added	
1:32	29	2		0.1336	0.450
1:38	35	8		0.1162	0.391
1:45	42	15		0.0972	0.327
1:50	47	20		0.0936	0.315
2:00	57	30		0.0918	0.309
2:08	65	38		0.0892	0.300
2:20	77	50		0.0876	0.295
2:50	107	80		0.085	0.286
2:55	112	85		0.0831	0.280
3:15	132	105		0.0828	0.279
3:21	138	111		0.0825	0.278
3:25	142	115		0.0819	0.276
3:30	147	120		0.082	0.276
3:31	148	121		0.0813	0.274
3:32	149	122		0.082	0.276
3:34	151	124	0	UV turned on	
3:43	160	133	9	0.0798	0.269
3:50	167	140	16	0.0763	0.257
4:12	189	162	38	0.0662	0.223
4:30	207	180	56	0.0591	0.199
4:45	222	195	71	0.0541	0.182

5:07	244	217	93	0.047	0.158
5:16	253	226	102	0.0443	0.149
5:30	267	240	116	0.0449	0.151
5:32	269	242	118	0.0404	0.136
5:33	270	243	119	0.0406	0.137
5:45	282	255	131	0.0365	0.123
6:00	297	270	146	0.0335	0.113
6:15	312	285	161	0.0299	0.101
7:00	357	330	206	0.0225	0.076
7:12	369	342	218	0.0206	0.069
7:15	372	345	221	0.0201	0.068
7:20	377	350	226	0.0196	0.066
7:25	382	355	231	0.0194	0.065

pH Attachment Beads - 2nd Trial	
MB Presence Time Elapsed (min)	LN (MB conc.)
0	
2	-0.8
8	-0.9
15	-1.1
20	-1.2
30	-1.2
38	-1.2
50	-1.2
80	-1.3
85	-1.3
105	-1.3
111	-1.3
115	-1.3
120	-1.3
121	-1.3
122	-1.3

124	
133	-1.3
140	-1.4
162	-1.5
180	-1.6
195	-1.7
217	-1.8
226	-1.9
240	-1.9
242	-2.0
243	-2.0
255	-2.1
270	-2.2
285	-2.3
330	-2.6
342	-2.7
345	-2.7
350	-2.7
355	-2.7

Uncoated Beads - 1st Trial			
Flow rate = 50 mL/min			
Time (pm)	Time Elapsed	Measured Absorbance	Concentration (mg/L)
3:20	0		0
3:22	2	0.0006	0
3:24	10 mL MB stock solution added		
3:25	5	0.1167	0.393
3:30	10	0.0921	0.310
3:35	15	0.0873	0.294
3:40	20	0.0855	0.288
3:45	25	0.0838	0.282
3:50	30	0.0835	0.281
3:51	UV turned on		
3:55	35	0.0826	0.278

4:00	40	0.0815	0.274
4:10	50	0.0806	0.271
4:20	60	0.079	0.266
4:30	70	0.0769	0.259
4:40	80	0.0764	0.257
4:50	90	0.0754	0.254
5:00	100	0.0742	0.250
5:10	110	0.0732	0.246
5:20	120	0.0724	0.244
System Shutdown			

Appendix C – System Pictures